

The island of deformation and shape co-existence in neutron-deficient nuclei of the Pb region using relativistic mean field model

M.S. Mehta[†], T.K. Jha[‡], S.K. Patra[§] and Raj K. Gupta[†]

[†] Department of Physics, Panjab University,
Chandigarh 160 014, India

[‡] P.G. Department of Physics, Sambalpur University,
Jyoti Vihar, Burla 768 019, India

[§] Institute of Physics, Sachivalaya Marg, Bhubaneswar 751 005, India.

Abstract:

We have investigated the ground-state structures of even-even neutron-deficient isotopes of Hg and Pb nuclei within the framework of a deformed relativistic mean field formalism for a number of commonly used parameter sets, namely NL1, NL3, NL-SH, NL-RA1 and TM1. The ground states of a bunch of Hg and Pb-isotopes towards the proton-dripline are found to be deformed for all the forces, with a constant pairing gap. The small differences in the ground- and the first-excited state binding energies predict a sea of low-lying excited states, and hence of shape co-existence, for both the Hg and Pb nuclei. In general, a discrepancy between the experimentally observed and theoretically predicted (sign of) quadrupole deformations is noticed in this mass region. The constrained potential energy surfaces and the single-particle energy spectra analyzed for some selected nuclei show that the known large shell gap for Pb nuclei at $Z=82$ is almost extinguished for its proton-rich isotopes.

PACS: 21.10.Dr, 21.10.Tg, 21.60.-n, 21.60.Fw

Keywords: Drip-line nuclei, binding energies, quadrupole deformations, single-particle energy spectra, relativistic mean field theory

1 Introduction

The study of the structures of Hg and Pb nuclei, in particular of the neutron-deficient isotopes, has been a puzzle and still remains a puzzle. A variety of structures have been proposed by different calculations, some questioning even the magicity of $Z=82$ shell for nuclei at the proton-drip line. Already in early 1970's, based on the Hartree-Fock (HF) calculation using Skyrme force, a shape transition from oblate to prolate in the ground-state of neutron-deficient Hg isotopes was reported with the decrease of mass number [1, 2, 3]. On the contrary, the later calculations based on the Strutinsky prescription with BCS pairing [4, 5] predicted an oblate ground-state for neutron-deficient Hg nuclei, agreeing with the experimental data on first excited 2^+ states.

The relativistic mean field (RMF) calculation for the neutron-deficient Hg and Pb nuclei was first made by one of us and collaborators in 1994 [6, 7], using the NL1 parameter set with the pairing interaction in BCS formalism, of constant gap parameters as in [8]. This calculation gave rather unexpected results. The ground-state shape of even-even $^{178,182,184,186}\text{Hg}$ was predicted to be prolate, and that of $^{184-196}\text{Pb}$ isotopes as deformed having co-existing prolate and oblate shapes. A further striking result was the superdeformed (SD) ground-state in ^{180}Hg . According to a critique by Heyde et al. [9], the above RMF results must be due to a particular choice of the force parameter and the very schematic treatment of pairing. In response to this comment, Takigawa et al. [10] showed that a reduction of the gap parameter for neutrons by a factor of two with NL1 force, or by changing the force to NL-SH set, the ground-state of ^{180}Hg does indeed changes from the superdeformed to one of the normal deformation. Depending on the strength of pairing gap for neutrons, it shifts from oblate to prolate, the SD state always remaining an excited state. However, for other neutron-deficient Hg and Pb nuclei, the change of the parameter set from NL1 to NL-SH did not alter much the predictions of either the prolate deformed ground-states of Hg or the deformed structures for Pb nuclei. However, another RMF calculation using NL3 force with BCS pairing shows all the neutron-deficient Pb nuclei to be spherical [11]. This means that the criticism of Heyde et al. [9] for the RMF predictions of Hg and Pb ground-state structures is answered only partially and the question of checking the sensitivity of RMF calculations to the choice of force parameter and/or the strength of pairing force needed further investigation.

Some further effort has been made for understanding the role of pairing strength in RMF calculations. Yoshida and Takigawa [12] have shown that a constant strength of the pairing interaction G (which makes the gap parameters strongly deformation de-

pendent), instead of constant gap parameters (independent of the deformations) with NL1 force itself reproduces the oblate shapes and charge radii of neutron-deficient Hg isotopes and restores the magicity of $Z=82$ shell for all the Pb isotopes. In addition, the isotope shifts of Pb isotopes are well reproduced. This makes one feel that the problem is settled once for all, if the results of this calculation will be independent of the choice of the force parameter set NL1 and the average gap parameters used for solving the pairing interaction equations for G . Instead, these authors suggested that, for exotic nuclei, the alternative, deformed relativistic Hartree-Bogoliubov (RHB) approach is superior to the BCS theory used by them, since it gives a unified description of both the mean-field and pairing correlations. Such a study is also taken up very recently by Nikšić et al. [13] for the ground state properties of neutron-deficient Pt, Hg and Pb nuclei, using the NL3 parameter set with finite range Gogny interaction DIS [14]. However, the results of this calculation opens up the problem once again, since they again predict $^{188-194}\text{Pb}$ nuclei as oblate deformed in their ground-states. Thus, in order to keep the magicity of $Z=82$ shell, a new parametrization, NL-SC, is proposed which takes into account the sizes of spherical shell gaps, particularly at $Z=82$, and hence reproduces the experimental data on binding energies, radii and ground-state deformations of these nuclei. However, such an effective interaction could not be considered as general and may not describe accurately the ground-state shapes of nuclei in other regions of shape co-existence.

The puzzle on structures of Hg and Pb nuclei at the proton-drip line is further complicated by the most recent large-scale mass measurements of proton-rich nuclei around $Z=82$ [15]. The reduction of two-proton separation energies [rather, the differences between two-proton separation energies of adjacent even-even nuclei with the same neutron number, $\delta_{2p} = S_{2p}(Z, N) - S_{2p}(Z + 2, N)$], for Pb nuclei with $N \approx 106$ [15], combined with the systematics of older measurements of Q_α -values and α -reduced widths [16], suggests the weakening of the spherical $Z=82$ shell for neutron number in between $N=82$ and 126. Using the non-relativistic self-consistent mean-field theory with Skyrme interaction or the RMF model with NL3 and NL-Z2 parameter sets in BCS approximation of pairing, Bender et al. [17] show that the systematics of δ_{2p} could well be described quantitatively in terms of the deformed ground states of Hg and Po isotopes. Already, a triple shape co-existence (spherical, oblate and prolate shapes of almost identical excitation energies) is observed in ^{186}Pb [18]. Also, the earlier calculations based on RMF approach show that the $Z=N=28$ loses its magicity for nuclei approaching the neutron dripline [19, 20] and that for the valley of superheavy nuclei the sequence of magic numbers is different from the

usual one [21]. These results make us believe that we could still learn much from the standard RMF model calculations, using the BCS formalism for pairing interaction, provided a systematic attempt is made for a number of parameter sets. We do this here for the parameter sets NL1, NL3, NL-SH, NL-RA1 and TM1, for the pairing gap parameters still taken from Madland and Nix [8]. This covers almost the entire range of the generally used force parameter sets for RMF model calculations. The case of zero pairing is also investigated. We find that some of the results do depend strongly on the choice of the parameter set. The already used parameter sets NL1, NL3 and NL-SH are also included here for the relative comparisons of the calculations made under similar conditions.

The paper is organised as follows: In section 2 we outline the essential formalism for the relativistic mean field Lagrangian. The results of our calculation for $^{170-200}\text{Hg}$ and $^{178-208}\text{Pb}$ nuclei are discussed in section 3. We look for the shape co-existence and possible deformation effects in this island of $Z=80$ and 82 nuclei. The ground-state and the first excited-state solutions are obtained for all the nuclei studied and the constrained potential energy surfaces (PES) are calculated for a few illustrative nuclei. For the deformation effects, the quadrupole deformation parameters and the single-particle energy spectra for both the spherical and deformed nuclei are analyzed. Finally a summary of our conclusions is added in section 4.

2 The formalism

In the last two decades, the RMF model has become known to be a very powerful tool to explain the properties of finite nuclei and infinite nuclear matter [22, 23, 24]. The RMF method has the advantage that, with proper relativistic kinematics and with the mesons and their properties already known or fixed from the properties of a few nuclei [23, 25, 26], the method gives excellent results for binding energies, root mean square (rms) radii, quadrupole and hexadecupole deformations and other nuclear properties, not only of spherical, but also of deformed nuclei. One of the major attractive features of the RMF formalism is that the spin-orbit strength and associated nuclear shell structure automatically arise from meson-nucleon interaction [27, 28].

We start with the relativistic Lagrangian density for a nucleon-meson many-body system,

$$\mathcal{L} = \overline{\psi}_i \{i\gamma^\mu \partial_\mu - M\} \psi_i + \frac{1}{2} \partial^\mu \sigma \partial_\mu \sigma - \frac{1}{2} m_\sigma^2 \sigma^2 - \frac{1}{3} g_2 \sigma^3 - \frac{1}{4} g_3 \sigma^4 - g_s \overline{\psi}_i \psi_i \sigma$$

$$\begin{aligned}
& - \frac{1}{4} \Omega^{\mu\nu} \Omega_{\mu\nu} + \frac{1}{2} m_w^2 V^\mu V_\mu + \frac{1}{4} c_3 (V_\mu V^\mu)^2 - g_w \bar{\psi}_i \gamma^\mu \psi_i V_\mu - \frac{1}{4} \vec{B}^{\mu\nu} \cdot \vec{B}_{\mu\nu} \\
& + \frac{1}{2} m_\rho^2 \vec{R}^\mu \cdot \vec{R}_\mu - g_\rho \bar{\psi}_i \gamma^\mu \vec{\tau} \psi_i \cdot \vec{R}^\mu - \frac{1}{4} F^{\mu\nu} F_{\mu\nu} - e \bar{\psi}_i \gamma^\mu \frac{(1 - \tau_{3i})}{2} \psi_i A_\mu. \quad (1)
\end{aligned}$$

The field for the σ -meson is denoted by σ , that for the ω -meson by V_μ and for the isovector ρ -meson by \vec{R}_μ . A^μ denotes the electromagnetic field. The ψ_i are the Dirac spinors for the nucleons whose third component of isospin is denoted by τ_{3i} . Here g_s , g_w , g_ρ and $\frac{e^2}{4\pi} = \frac{1}{137}$ are the coupling constants for σ , ω , ρ mesons and photon, respectively. g_2 , g_3 and c_3 are the parameters for the nonlinear terms of σ - and ω -mesons. M is the mass of the nucleon and m_σ , m_ω and m_ρ are the masses of the σ , ω and ρ -mesons, respectively. $\Omega^{\mu\nu}$, $\vec{B}^{\mu\nu}$ and $F^{\mu\nu}$ are the field tensors for the V^μ , \vec{R}^μ and the photon fields, respectively [26].

From the relativistic Lagrangian we get the field equations for the nucleons and mesons. These equations are solved by expanding the upper and lower components of Dirac spinors and the Boson fields in a deformed harmonic oscillator basis with an initial deformation. The set of coupled equations is solved numerically by a self-consistent iteration method. The centre-of-mass motion is estimated by the usual harmonic oscillator formula $E_{c.m.} = \frac{3}{4}(41A^{-1/3})$. The quadrupole deformation parameter β_2 is evaluated from the resulting quadrupole moment [26] using the formula,

$$Q = Q_n + Q_p = \sqrt{\frac{9}{5\pi}} A R^2 \beta_2, \quad (2)$$

where $R = 1.2A^{1/3}$. The total binding energy of the system is,

$$E_{total} = E_{part} + E_\sigma + E_\omega + E_\rho + E_c + E_{pair} + E_{c.m.}, \quad (3)$$

where E_{part} is the sum of the single-particle energies of the nucleons and E_σ , E_ω , E_ρ , E_c and E_{pair} are the contributions of the mesons fields, the Coulomb field and the pairing energy, respectively. For the open shell nuclei, the effect of pairing interactions is added in the BCS formalism. The pairing gaps for proton Δ_p and neutron Δ_n are calculated from the relations [8],

$$\begin{aligned}
\Delta_p &= r b_s Z^{-1/3} e^{(sI - tI^2)} \\
\Delta_n &= r b_s N^{-1/3} e^{-(sI + tI^2)} \quad (4)
\end{aligned}$$

where $r = 5.72 \text{ MeV}$, $s = 0.118$, $t = 8.12$, $b_s = 1$ and $I = (N - Z)/(N + Z)$.

3 Results and Discussions

In this section, we discuss the results of our relativistic mean field calculations. The commonly used NL1 [29], NL-SH [30], NL3 [31, 32], TM1 [33] and the more recent

NL-RA1 [34] parameter sets are employed for the present calculations. For the NL3 parameter set, we have used the numerical data from [32], which is slightly different (in decimal places) from that given in their earlier work [31] and used in later work [11] mentioned in the Introduction; this rounding off of the numbers makes a difference of about 1 MeV in the total binding energy. We display our results in Table 1 for only some Hg and Pb isotopes, where the experimental data (on both the binding energy and deformation parameter) are available, and discuss the complete calculations for $^{170-200}\text{Hg}$ and $^{178-208}\text{Pb}$ nuclei in Figs. 1-5.

In Table 1, we notice that the calculated binding energies BE and quadrupole deformation parameters β_2 , for both the cases of with and without pairing, are quite close to the experimental values, taken from Refs. [35, 36]. Also, interesting enough, all the parameter sets give almost similar results. A closer inspection of Table 1 shows that NL3 and NL-RA1 sets are somewhat better than the other parameter sets for predicting the experimental binding energies, NL3 being superior in some cases and NL-RA1 in some other cases. Note that the evaluation of quadrupole deformation parameter β_2 from the experimental $B(E2)$ -value [36] gives only the absolute β_2 -value and hence the comparison between the calculated β_2 and experimental β_2 is limited in this respect of the sign.

In Fig. 1, the difference ΔE of the binding energies between the intrinsic ground-state and the intrinsic first excited-state (from here onwards, referred to simply as the ground-state and excited-state) is shown for Hg and Pb isotopes. The upper and lower panels show without and with pairing interaction, respectively. Almost all the Hg isotopes (without pairing, upper panel) show very small energy difference between the ground- and first excited-states, i.e. without pairing effects, ΔE is within ~ 1.5 MeV for almost all the Hg nuclei with all the parameter sets used. The main exception is ^{184}Hg , where $\Delta E \approx 3.5$ MeV for almost all the parameter sets. The other notable cases are ^{186}Hg for NL-SH, $^{194,196}\text{Hg}$ for NL1 and ^{188}Hg for TM1 force, where $\Delta E > 2$ MeV. Hence, in general, for the Hg nuclei considered here, we could say that the first excited-state is not far from the ground-state, a result very much consistent with the earlier theoretical predictions [1, 39, 40]. Similarly, in the case of Pb isotopes (without pairing, upper panel), the difference ΔE is also within ≈ 1.5 MeV for most of the nuclei, in particular for $^{178-192}\text{Pb}$ and $^{200,202,206,208}\text{Pb}$ nuclei for all the parameter sets. The notable exception is the TM1 force for $^{178,180}\text{Pb}$ and $^{200-208}\text{Pb}$ where ΔE is much larger. For $^{178-188}\text{Pb}$ and $^{206,208}\text{Pb}$, the ΔE is very small, ~ 0.8 MeV or less. In $^{194,196}\text{Pb}$ nuclei, the difference ΔE is more than 1.5 MeV for almost all the parameter sets. Thus, once again, with a few exceptions, the ground-states and the first excited-

states for the Pb nuclei investigated here are nearly degenerate. In other words, with zero (or week) pairing there are low-lying excited-state solutions or shape co-existing states in the island of Hg and Pb nuclei.

In the lower panel we plot the same ΔE , but for including the pairing effects. A comparison between two (upper and lower) panels allows us to see the influence of pairing correlations (note the difference in the ordinate scales of the two panels). In general terms, we notice that the pairing interaction has very little effect on the ground- and excited-state energies in Hg and Pb nuclei. For example, $^{170-180,190,198,200}\text{Hg}$ and nearly all Pb nuclei, for most of the forces, have the energy difference ΔE less than 1.5 MeV. The notable exceptions are $^{182-188}\text{Hg}$ and $^{194-198}\text{Pb}$ isotopes, which also have $\Delta E \leq 2.7$ MeV, for many parameter sets.

In order to get a better realization of the barrier between the ground- and excited-states, we have plotted the potential energy surfaces (PES) in Fig. 2 for two illustrative, strongly deformed nuclei, ^{180}Hg and ^{186}Pb . This is a constrained calculation where, instead of minimizing $\langle H_0 \rangle$, we have minimised $\langle H - \lambda Q \rangle$, with λ as a Lagrange multiplier and Q , the quadrupole moment [41]. This gives us the binding energy as a function of the quadrupole deformation parameter β_2 . In Fig. 2, we observe that there is a low-lying solution near to the ground-state for both ^{180}Hg and ^{186}Pb nuclei. The two solutions have about the same energy difference of ~ 3 MeV for both ^{180}Hg and ^{186}Pb nuclei, and for all the parameter sets. Thus, the shape co-existence seems to be nearly independent of the chosen parameter sets. It may be noted that the (multiple) shape co-existence is a very well studied phenomenon in Pb nuclei [42] and, as already mentioned above, with ^{186}Pb as the best studied case, having three differently shaped 0^+ states observed recently [18]. However, the present RMF calculations do not give the observed spherical solution for ^{186}Pb nucleus.

Fig. 3 gives the variation of the quadrupole deformation parameter β_2 as a function of mass number A , for the two cases of, respectively, without and with (upper and lower panel) pairing interactions. In the upper panel (without pairing) for Hg-isotopes all forces show the same transition of shape with the mass number. This transition is nearly independent of adding the pairing strength (compare the upper and lower panels for Hg nuclei). Thus, for Hg nuclei, we notice no significant change for adding the pairing interaction, but for Pb nuclei, for all the parameter sets, we observe that the pairing has a very significant effect on their ground state structures. The oblate shape for $^{182-190}\text{Pb}$ nuclei becomes prolate when pairing is added. This happens because the first excited-states are very close to the ground-states for these nuclei (see Fig. 1) and a small change in the input parameters, like for the pairing strength,

can flip the ground-state solution into an excited-state or vice versa.

For Hg nuclei, almost independent of pairing strength, the maximum (prolate) quadrupole deformation is for ^{184}Hg ($\beta_2=0.30\text{--}0.33$ for the five parameter sets used), and for $^{170\text{--}176}\text{Hg}$, the the ground-state shape is spherical (near spherical) with all the forces. The change in shape from prolate to oblate takes place at mass number $A=188$ for NL1, at $A=190$ for the other three parameter sets, while TM1 shows this change a still further at $A=192$. In other words, the $^{178\text{--}188}\text{Hg}$ nuclei are prolate deformed for all the parameter sets used. In the experiments [40], however, the estimated prolate-oblate energy differences for $^{184\text{--}188}\text{Hg}$ nuclei allow these authors to conclude that the lower of the co-existence states is an oblate one and the other low-lying stable prolate solution is the excited state, supporting the earlier theoretical results of Bengtsson et al. [4] using Woods-Saxon potential and another RMF calculation [11] using the (older) NL3 parameter set of Ref. [31]. Note, however, that we have used here the more recent NL3 parameter constants of Ref. [32] and, as already mentioned above, the results of two NL3 parameter sets (old and recent) could differ by about 1 MeV, which is of the order of ΔE for some of these nuclei (see Fig. 1) and hence may change the prolate solution to oblate one. On the other hand, for Pb nuclei, with pairing effects included (lower panel), we notice a change from spherical to oblate deformation, right at the begining for ^{180}Pb or ^{182}Pb , depending on the parameter set used, and again from oblate to prolate region at ^{180}Pb or ^{182}Pb . The nuclei $^{182\text{--}190}\text{Pb}$ are prolate for all sets. Alternatively, with pairing effects switched off (upper panel), almost all the Pb nuclei studied here are oblate deformed with $\beta \sim 0.2$. In particular, our predictions for $^{192,194}\text{Pb}$, e.g. $\beta_2=-0.172$ and -0.166 for NL3 set, are in excellent agreement with the experimental data ($\beta_2=-0.18$, -0.175 and -0.17 [37]) where the sign of β_2 is determined on the basis of a theoretical calculation [38]. However, we consider the neutron deficient $^{182\text{--}190}\text{Pb}$ as prolate deformed, advocating strong pairing correlations, since the neighbouring $^{178\text{--}188}\text{Hg}$ nuclei are prolate deformed, independent of pairing as well as parameters of the forces used.

Next, Figs. 4 and 5 (with and without pairing, respectively) display the single-particle spectra for two illustrative nuclei ^{186}Pb and ^{208}Pb , i.e. the most deformed and the most spherical isotopes of the chosen series, for the representative NL1 and NL3 parameter sets. The results obtained for the other parameter sets NL-SH, NL-RA1 and TM1 are similar. From Fig. 4 (where pairing effects are included), we notice that the shell gap for the spherical nucleus ^{208}Pb is well distinguished at $Z=82$ (and at $N=126$), which in the deformed nucleus ^{186}Pb seems to have been reduced considerably, both for protons and neutrons (more so for protons). All the

four parameter sets show almost the same result. We have also repeated our analysis for the case of not including the pairing interactions (Fig. 5) and found that there is no appreciable change in the shell gaps, except that for the deformed ^{186}Pb nucleus the gap at $Z=82$ is now larger ~ 2 MeV (for NL1 force), to be compared with ~ 4 MeV for the spherical ^{208}Pb nucleus. Thus, we can say that some light, neutron-deficient isotopes of Pb are deformed and show the signatures of gap reduction, as is observed in the experiments of Toth et al. [16]. It may be noted here that if the single particle energy shell gap near the magic shell is larger than the two-nucleon interaction strength, then the shell gap at the closed shell has to be considered. On the other hand, for a shell gap smaller than the two-nucleon interaction matrix, the considered nucleon can jump from this shell to the higher orbits.

Finally, a few words about the co-existing SD state as the ground-state, predicted in Refs. [6, 7] for ^{180}Hg using NL1 parameter set with full BCS pairing gap parameter from Ref. [8]. In order to verify this result, we have repeated this calculation by using NL1, NL-SH, NL3 and NL-RA1 parameter sets by increasing the oscillator shell number to $N_F = N_B = 16$. The shapes of both the normal and super-deformed solutions are investigated, by taking the cases of both with and without pairing interactions into account. For the NL1 parameter set with pairing, the binding energy BE=1420.420 MeV (at $\beta_2=0.569$) for the SD solution, and the BE=1422.405 MeV for normal deformation ($\beta_2 = 0.323$). For the case of without pairing, the binding energy (and deformation parameter) for the normal and SD configurations are BE=1420.304 ($\beta_2 = 0.328$) and BE=1420.420 MeV ($\beta_2 = 0.569$), respectively. This means that in ^{180}Hg for NL1 parameter set, the SD solution is very close to the ground-state and could be the ground-state solution itself, as was suggested by the earlier calculations [6, 7] based on NL1 parameter set. However, for the other three parameter sets we notice in Table 2 that the normal and SD solutions are rather far apart. Hence, the NL1 parameter set seems to have the special feature of predicting a shape co-existing super-deformed state with the ground-state, contrary to other parameter sets NL-SH, NL3 and NL-RA1 studied here.

4 Summary and Conclusions

In the present investigation we have calculated the binding energy, the single-particle energy spectrum and the quadrupole deformation parameter β_2 for some neutron-deficient Hg and Pb isotopes, using the deformed relativistic mean field formalism with the commonly employed parameter sets NL1, NL3, NL-SH, TM1 and NL-RA1. We

find a low-lying excited-state in most of the chosen nuclei, for all the five parameter sets. Thus, the shape co-existence in neutron-deficient Hg and Pb nuclei is predicted to be nearly independent of the force parameters and pairing correlations. Also, clear deformed structures for the neutron-deficient $^{178-188}\text{Hg}$ and $^{182-190}\text{Pb}$ isotopes are noticed, irrespective of the chosen parameter set, due to melting away of the usual $Z=82$ shell closure.

For the binding energy comparisons with experiments, the NL3 and NL-RA1 parameters have a slight edge over the other parameter sets. The potential energy surfaces are investigated with all the five forces by taking the extremely deformed ^{180}Hg and ^{186}Pb nuclei as the representative cases. Both the nuclei show a similar behavior for each parameter set. The single-particle energy spectrum shows a large shell gap at $Z=82$ (and also at $N=126$) for the most spherical nucleus ^{208}Pb , but the same is not true for the most deformed ^{186}Pb . For the deformed nucleus the shell gap at $Z=82$ is reduced considerably.

Concluding, we emphasize that a bunch of Hg and Pb nuclei in the considered island of Hg and Pb nuclei are deformed and that the magic character at $Z=82$ is lost for the neutron-deficient deformed Pb nuclei. The discrepancy between the deformed RMF predictions and the experiments for the quadrupole deformation is due to the low-lying excited states (shape coexistence) obtained in these nuclei. Apparently, to reproduce the experimental data, it is essential to perform a more careful calculation.

Acknowledgements

We thank Prof. A. Ansari for a careful reading of the manuscript and for many valuable suggestions. One of us (RKG) is grateful to the Department of Science and Technology, Govt. of India for support of this research work in terms of a Sr. Research Scientistship to him. MSM and TKJ thank the Institute of Physics, Bhubaneswar, for the kind hospitality during the completion of this work.

Figure Captions

Figure 1: The deformed RMF calculated difference between the ground- and first excited-state binding energies as a function of the mass number A for various Hg and Pb isotopes, without (upper panel) and with (lower panel) pairing interaction.

Figure 2: The deformed RMF calculated potential energy surfaces for the most deformed ^{180}Hg and ^{186}Pb nuclei, both with pairing (upper panel) and without pairing (lower panel), using five parameter sets.

Figure 3: The quadrupole deformation parameter as a function of the mass number A for Hg and Pb nuclei, calculated on deformed RMF model with pairing (upper panel) and without pairing (lower panel) interactions.

Figure 4: The single-particle energy spectra for the most spherical ^{208}Pb and deformed ^{186}Pb nuclei, calculated on deformed RMF model for NL1 and NL3 parameter sets. Pairing interaction is included here.

Figure 5: Same as for Fig. 4 but for without pairing interaction.

References

- [1] A. Faessler, U. Götz, B. Slavov, and T. Ledergerber, Phys. Lett. **B39**, 579 (1972).
- [2] M. Cailliau, J. Leterrier, H. Flocard, and P. Quentin, Phys. Lett. **B46**, 11 (1973).
- [3] D. Kolb and C. Y. Wong, Nucl. Phys. **A245**, 205 (1975).
- [4] R. Bengtsson, et al., Phys. Lett. **B183**, 1 (1987).
- [5] W. Nazarewicz, Phys. Lett. **B305**, 195 (1993).
- [6] S.K. Patra, S. Yoshida, and N. Takigawa, Phys. Rev. **C50**, 1924 (1994).
- [7] S. Yoshida, S.K. Patra, N. Takigawa, and C.R. Praharaj, Phys. Rev. **C50**, 1398 (1994).
- [8] D.G. Madland and J.R. Nix, Nucl. Phys. **A476**, 1 (1988);
P. Möller and J.R. Nix, At. Data Nucl. Data Tables **39**, 213 (1988).
- [9] K. Heyde, C. De Coster, P. van Druppen, M. Huyse, J. L. Wood, and W. Nazarewicz, Phys. Rev. **C53**, 1035 (1996).
- [10] N. Takigawa, S. Yoshida, K. Hagino, and S. K. Patra, Phys. Rev. **C53**, 1038 (1996).
- [11] G.A. Lalazissis, S. Raman and P. Ring, At. Data and Nucl. Data Tables, **71**, 1 (1999).
- [12] S. Yoshida and N. Takigawa, Phys. Rev. **C55**, 1255 (1997).
- [13] T. Nikšić, D. Vretenar, P. Ring, and G.A. Lalazissis, Phys. Rev. **C65**, 054320 (2002).
- [14] J.F. Berger, M. Girod, and D. Gogny, Nucl. Phys. **A428**, 32 (1984).
- [15] Yu. N. Novikov et al. Nucl. Phys. **A697**, 92 (2002).
- [16] K.S. Toth et al. Phys. Rev. **C60**, 011302(R) (1999).
- [17] M. Bender, T. Cornelius, G.A. Lalazissis, J.A. Maruhn, W. Nazarewicz, and P.-G. Reinhard, Eur. Phys. J. **A14**, 23 (2002).

- [18] A.N. Andreyev, et al., *Nature* **405**, 430 (2000).
- [19] R.K. Gupta, S.K. Patra and W. Greiner, *Mod. Phys. Lett. A* **12**, 1317 (1997);
S.K. Patra, R.K. Gupta and W. Greiner, *Int. J. Mod. Phys. E* **6**, 641 (1997).
- [20] T.R. Werner, et al., *Phys. Lett. B* **335**, 259 (1994);
T.R. Warner, et al., *Nucl. Phys. A* **597**, 327 (1996).
- [21] S.K. Patra, W. Greiner and R.K. Gupta, *J. Phys. G: Nucl. Part. Phys.* **26**, L65 (2000); *ibid* **26**, 1569 (2000).
- [22] R. Machleidt, *Adv. Nucl. Phys.* **19**, 189 (1989).
- [23] S.K. Patra and C.R. Praharaj, *Phys. Rev. C* **44**, 2552 (1991).
- [24] M. Del Estal, M. Centelles, X. Viñas and S.K. Patra, *Phys. Rev. C* **63**, 024314 (2001).
- [25] M. Rufa, P.-G. Reinhard, W. Greiner and M.R. Stranger, *Phys. Rev. C* **38**, 390 (1988);
P.-G. Reinhard, *Z. Phys. A* **329**, 257 (1993).
- [26] Y.K. Gambhir, P. Ring and A. Thimet, *Ann. Phys.* **198**, 132 (1990).
- [27] C.J. Horowitz and B.D. Serot, *Nucl. Phys. A* **368**, 503 (1981).
- [28] B.D. Serot and J.D. Walecka, *Adv. Nucl. Phys.* **16**, 1 (1986).
- [29] P.-G. Reinhard, M. Rufa, J. Maruhn, W. Greiner, and J. Friedrich, *Z. Phys. A* **323**, 13 (1986).
- [30] M.M. Sharma, M.A. Nagarajan, and P. Ring, *Phys. Lett. B* **312**, 377 (1993).
- [31] G.A. Lalazissis, J. König, and P. Ring, *Phys. Rev. C* **55**, 540 (1997).
- [32] M.M. Sharma, A.R. Farhan, and S. Mythili, *Phys. Rev. C* **61**, 054306 (2000).
- [33] Y. Sugahara and H. Toki, *Nucl. Phys. A* **579**, 557 (1994).
- [34] M. Rashdan, *Phys. Rev. C* **63**, 044303 (2001).
- [35] S. Raman, et al., *At. Data Nucl. Data Tables* **36**, 1 (1987).

- [36] G. Audi, O. Berstllon, J. Blachot and A.H. Webpstra, Nucl. Phys. **A624**, 1 (1997).
- [37] P. Dendooven, et al., Phys. Lett. **B226**, 27 (1989).
- [38] R. Bengtsson and W. Nazarewicz, Lund-Mph-87/08 preprint.
- [39] S. Frauendorf and V.V. Pashkevich, Phys. Lett. **B55**, 365 (1975).
- [40] G.D. Dracoulis, et al., Phys. Rev. **B208**, 365 (1988).
- [41] S.K. Patra, B.K. Raj, M.S. Mehta and R.K. Gupta, Phys. Rev. **C65**, 054323 (2002).
- [42] R. Julin, et al., J. Phys. G: Nucl. Part. Phys. **27**, R109 (2001).

Table 1: The ground-state binding energy BE and the quadrupole deformation parameter β_2 of some Hg and Pb isotopes for the five parameter sets, compared with experimental (or extrapolated) data [36]. The binding energy is in MeV.

Nuclei	Sets	BE	BE	BE(expt.)	β_2	β_2	β_2 (expt.)
		without pairing	with pairing		without pairing	with pairing	
^{184}Hg	NL1	1458.7	1460.4	1448.7	0.317	0.327	0.156[35]*
	NL3	1452.3	1453.9		0.306	0.320	
	NL-SH	1456.8	1458.8		0.295	0.304	
	NL-RA1	1448.8	1450.5		0.304	0.319	
	TM1	1455.8	1457.6		0.308	0.325	
^{186}Hg	NL1	1476.0	1478.4	1467.1	0.307	0.289	0.131[35]*
	NL3	1469.6	1471.7		0.296	0.311	
	NL-SH	1474.7	1476.9		0.289	0.301	
	NL-RA1	1466.1	1468.4		0.297	0.312	
	TM1	1472.6	1475.0		0.297	0.321	
^{196}Hg	NL1	1554.1	1555.1	1551.3	-0.151	-0.139	0.116[35]
	NL3	1550.9	1552.1		-0.139	-0.137	
	NL-SH	1555.0	1556.6		-0.117	-0.124	
	NL-RA1	1546.9	1548.3		-0.137	-0.134	
	TM1	1550.1	1551.6		-0.141	-0.148	
^{198}Hg	NL1	1567.8	1569.0	1566.5	-0.135	-0.120	0.107[35]
	NL3	1566.3	1567.5		-0.128	-0.124	
	NL-SH	1571.1	1572.3		-0.103	-0.115	
	NL-RA1	1562.6	1564.0		-0.127	-0.122	
	TM1	1564.8	1566.2		-0.130	-0.134	
^{200}Hg	NL1	1581.4	1583.7	1581.2	-0.120	-0.096	0.098[35]
	NL3	1581.8	1583.7		-0.111	-0.109	
	NL-SH	1586.8	1588.6		-0.106	-0.110	
	NL-RA1	1578.4	1580.3		-0.109	-0.112	
	TM1	1579.45	1580.3		-0.113	-0.109	
^{190}Pb	NL1	1498.9	1500.8	1489.7	-0.194	-0.188	-0.180[37]
	NL3	1491.4	1493.2		-0.195	0.289	
	NL-SH	1495.9	1497.0		-0.183	0.268	
	NL-RA1	1487.4	1488.5		-0.192	0.289	
	TM1	1493.9	1496.6		-0.195	0.297	
^{192}Pb	NL1	1516.2	1518.0	1508.1	-0.193	-0.182	-0.175[37]
	NL3	1509.2	1510.9		-0.182	-0.173	
	NL-SH	1513.9	1515.0		-0.175	-0.162	
	NL-RA1	1504.9	1506.4		-0.180	-0.170	
	TM1	1511.3	1513.2		-0.182	-0.181	
^{194}Pb	NL1	1533.2	1534.7	1526.0	-0.181	-0.175	-0.170[37]
	NL3	1526.6	1528.3		-0.173	-0.166	
	NL-SH	1531.0	1532.5		-0.165	-0.156	
	NL-RA1	1522.4	1523.9		-0.173	-0.164	
	TM1	1528.3	1530.1		-0.173	-0.171	

* In [38], $\beta_2=0.26$, 0.25 respectively.

Table 1: Continued...

Nuclei	Sets	BE	BE	BE(expt.)	β_2	β_2	β_2 (expt.)
		without pairing	with pairing		without pairing	with pairing	
^{204}Pb	NL1	1610.8	1612.3	1607.5	0.027	0.000	0.041[35]
	NL3	1609.1	1610.0		0.027	0.000	
	NL-SH	1612.9	1613.9		0.025	0.000	
	NL-RA1	1604.9	1606.0		0.026	0.000	
	TM1	1604.8	1608.1		0.027	0.006	
^{206}Pb	NL1	1627.0	1627.5	1622.4	0.000	0.000	0.032[35]
	NL3	1625.4	1625.8		0.000	0.000	
	NL-SH	1628.6	1629.1		0.000	0.000	
	NL-RA1	1621.1	1621.6		0.000	0.000	
	TM1	1619.5	1622.9		0.051	0.004	
^{208}Pb	NL1	1641.6	1641.2	1636.5	0.000	0.000	0.054[35]
	NL3	1640.5	1640.1		0.000	0.000	
	NL-SH	1642.6	1642.7		0.000	0.000	
	NL-RA1	1635.8	1635.8		0.000	0.000	
	TM1	1636.3	1636.6		0.002	0.003	

Table 2: For ^{180}Hg , the binding energy BE and quadrupole deformation parameter β_2 for normal and superdeformed bands, computed on deformed RMF model with and without pairing interaction, using various parameter sets.

Nucleus	Sets	BE	β_2	BE	β_2	shape
		with pairing		without pairing		
^{180}Hg	NL1	1422.405	0.323	1420.304	0.328	normal
		1420.420	0.569	1420.420	0.569	superdeformed
	NL-SH	1420.811	0.307	1418.323	0.284	normal
		1411.157	0.955	1412.829	0.598	superdeformed
	NL3	1414.833	0.317	1412.387	0.293	normal
		1410.907	0.572	1409.437	0.605	superdeformed
	NL-RA1	1411.593	0.318	1409.189	0.291	normal
		1407.188	0.583	1405.702	0.606	superdeformed

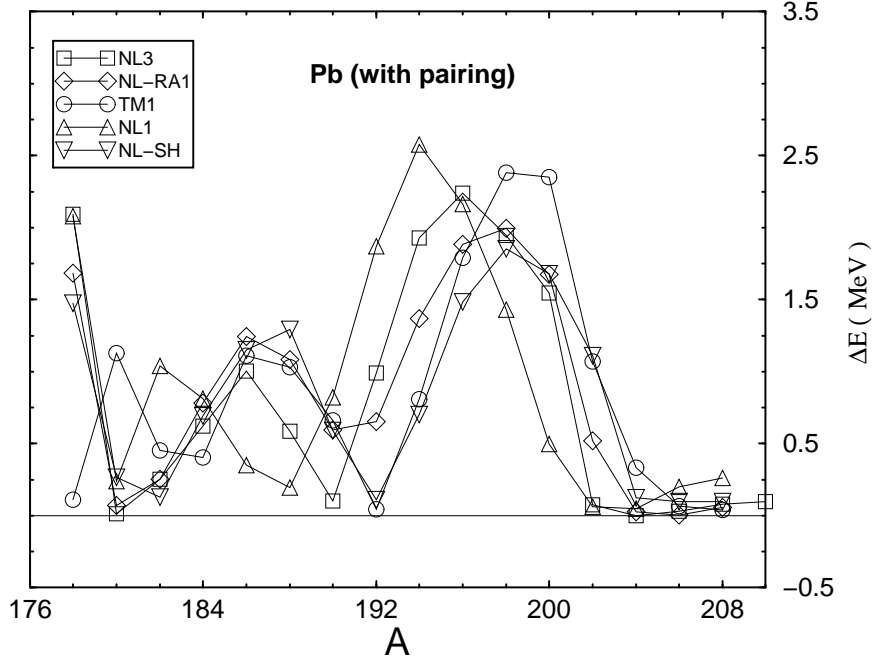
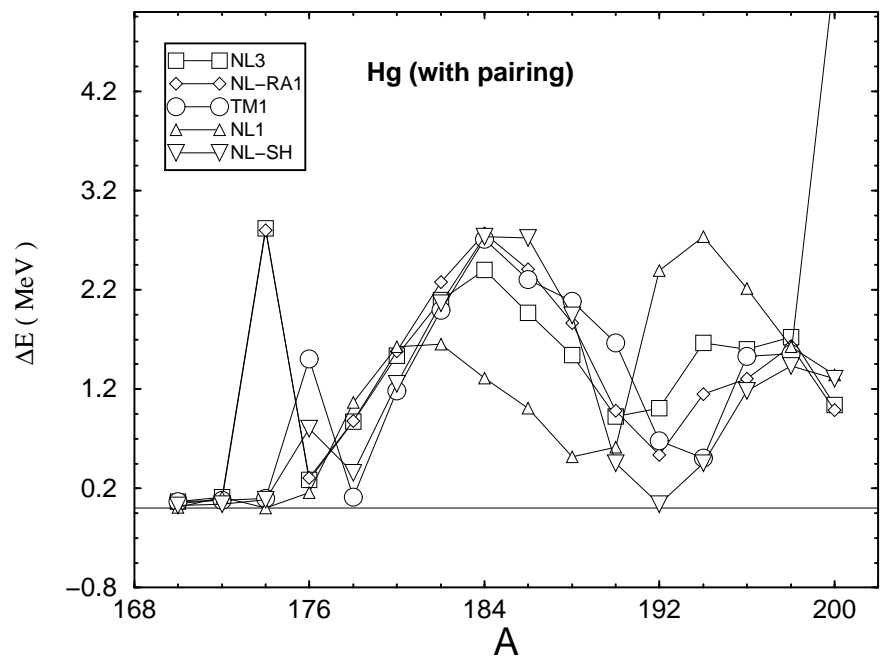
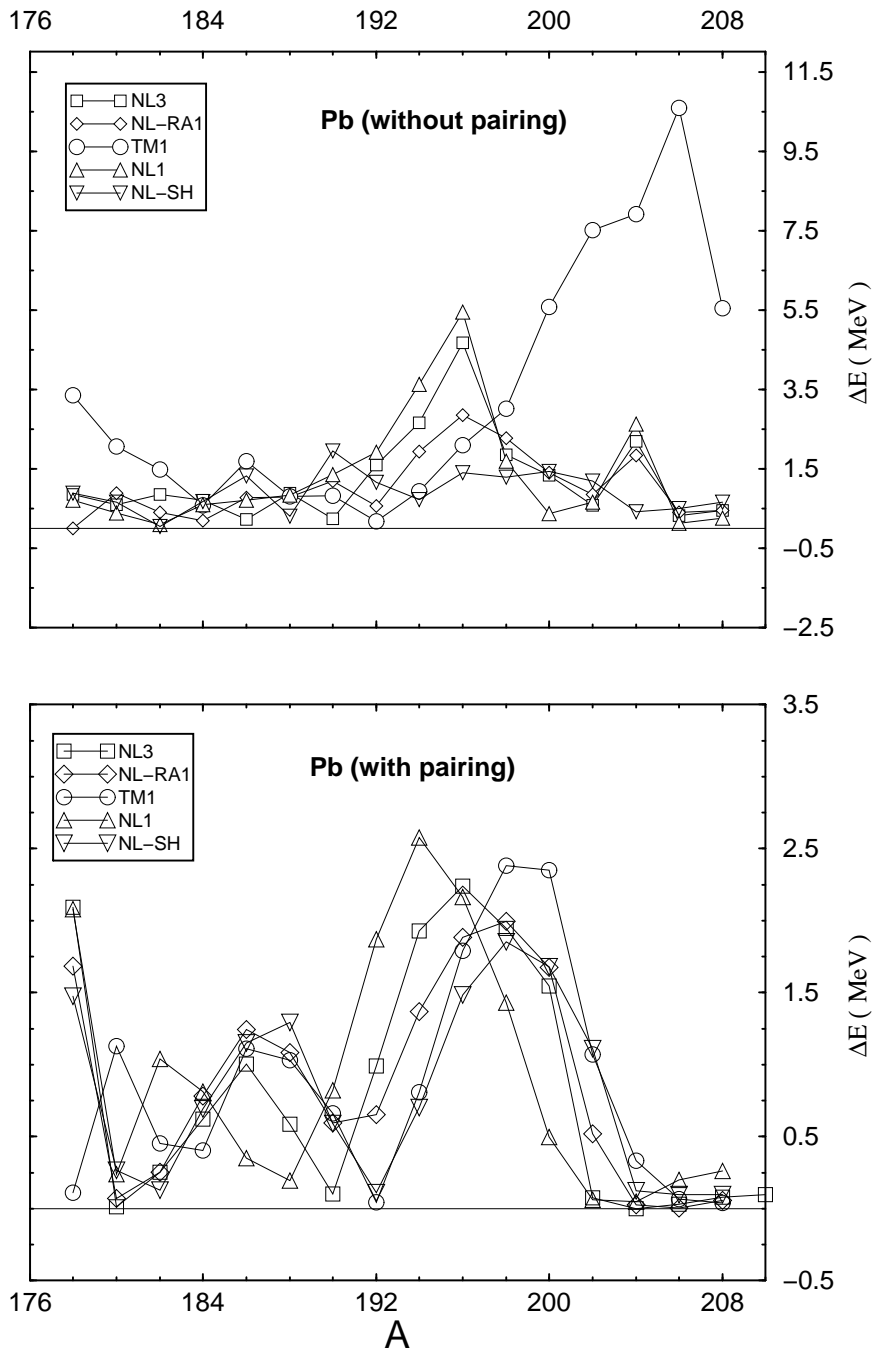
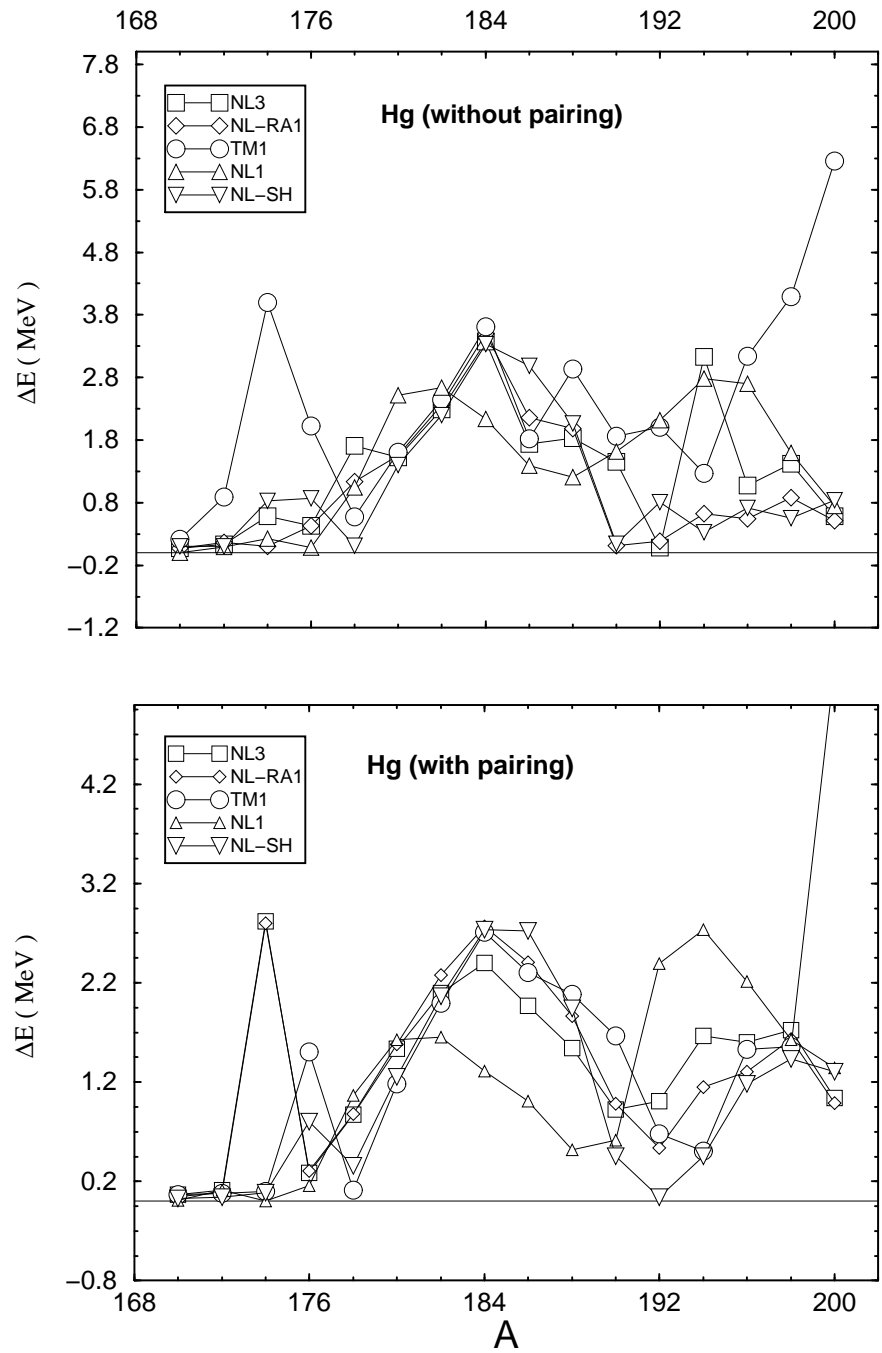


fig. 1

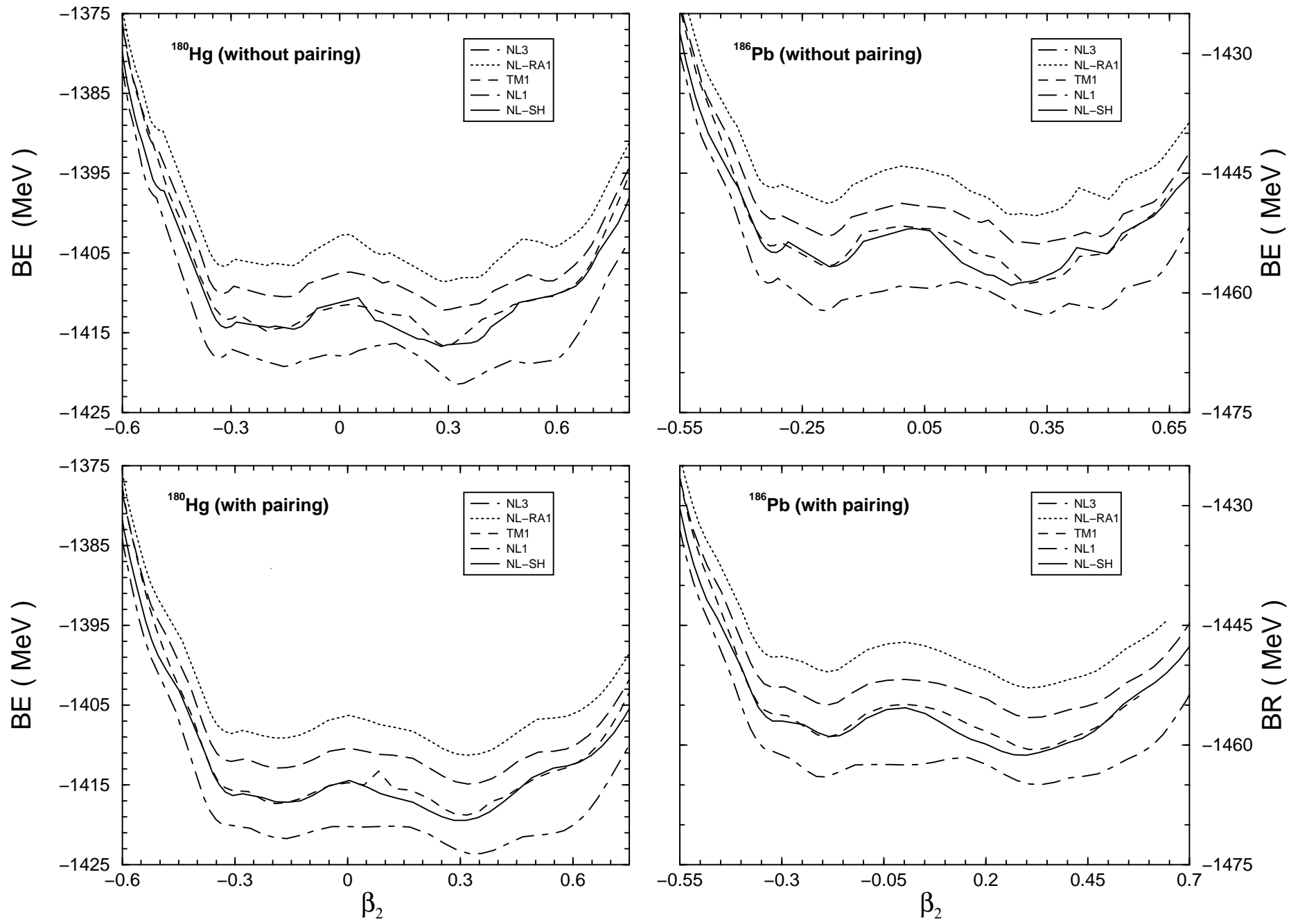


fig. 2

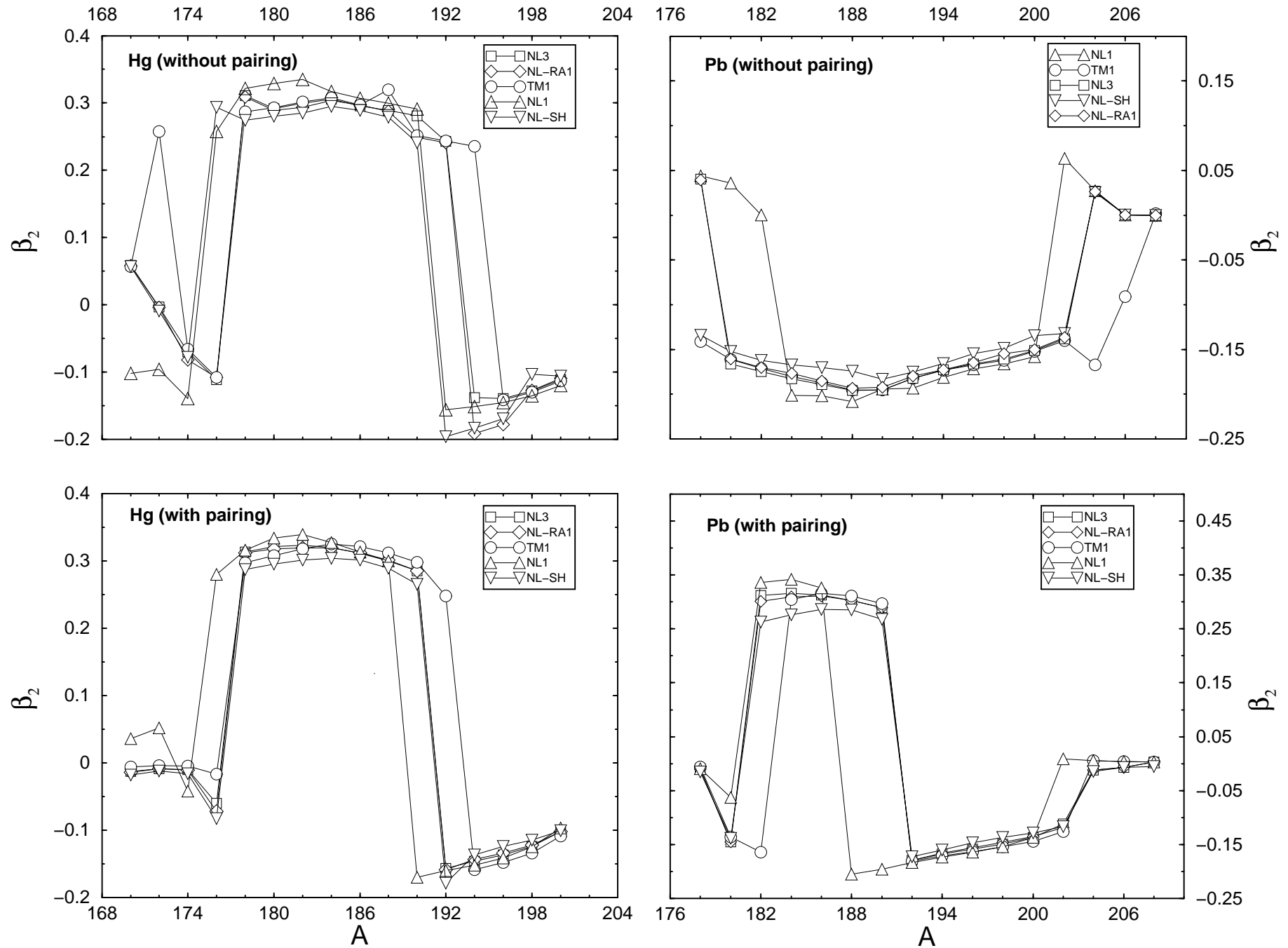


fig. 3

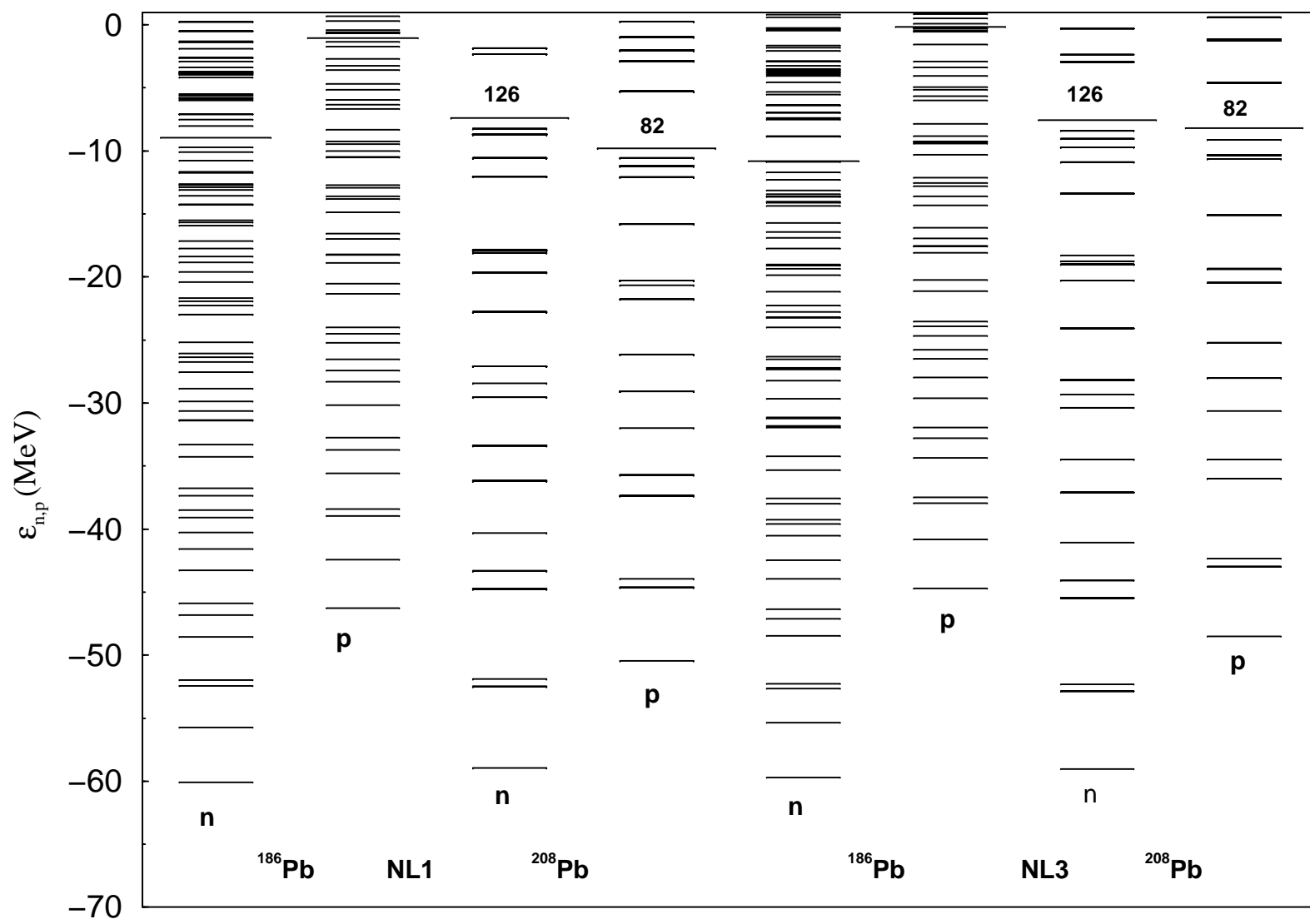


fig. 4

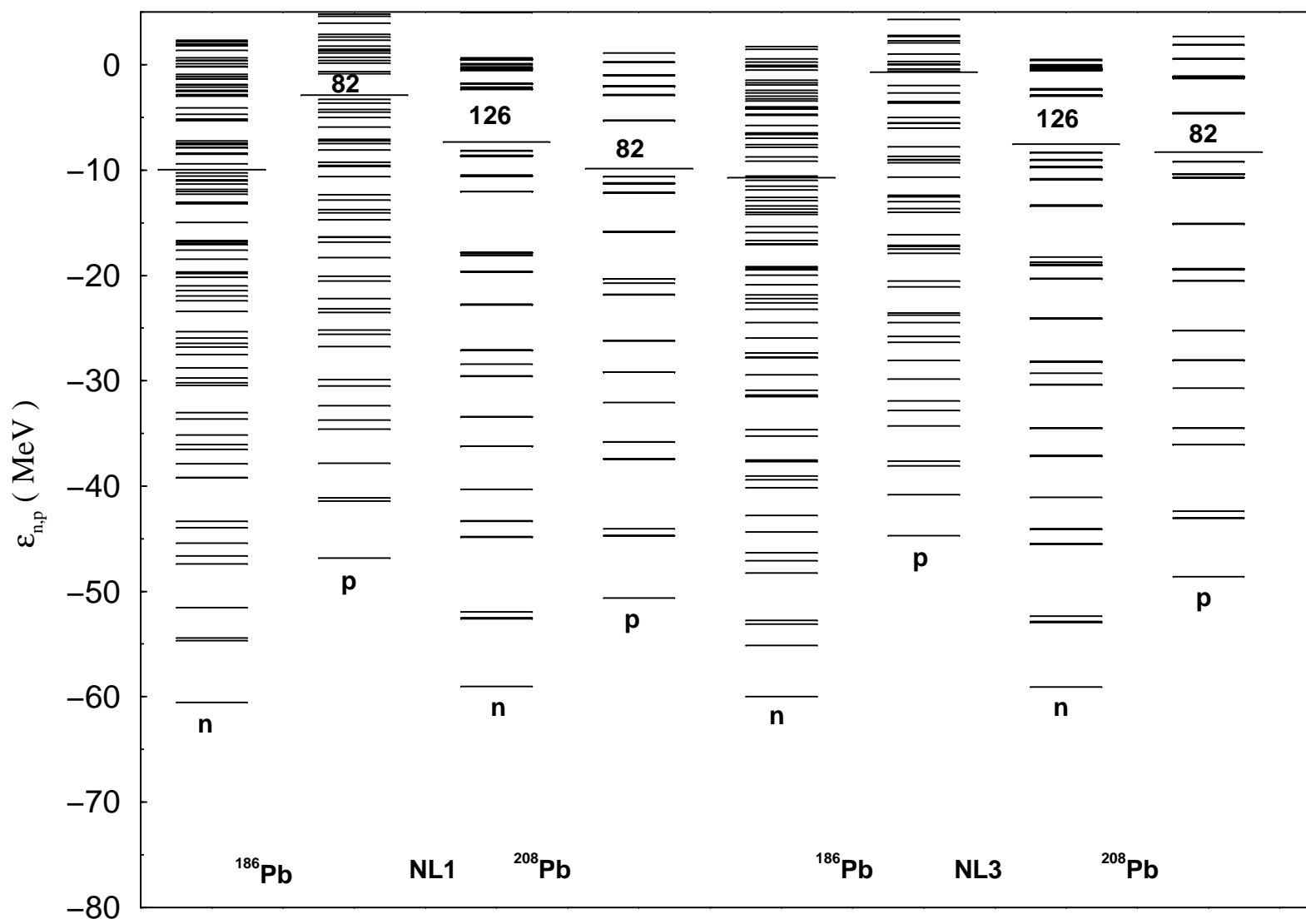


fig. 5